FIRST RESULTS ON CHARGED PARTICLE PRODUCTION IN ALICE EXPERIMENT AT LHC*

Marek Kowalski

for the ALICE Collaboration

Institute of Nuclear Physics Polish Academy of Sciences
Radzikowskiego 152, 31-342 Kraków, Poland

(Received December 22, 2010)

The ALICE experiment is the dedicated heavy-ion experiment at the CERN LHC, but its physics program also covers *pp* physics. ALICE, since its start, has collected *pp* data at 3 different center-of-mass energies — 900 GeV, 2.36 TeV and 7 TeV. Here, a brief description of the experimental apparatus is given, and some recent results on the particle multiplicity and charged particle spectra are presented. Results are compared with the existing data from lower energies and with Monte Carlo predictions.

DOI:10.5506/APhysPolB.42.859
PACS numbers: 13.75.Cs

1. Introduction

Although ALICE's main goal is the search and study of the new state of matter — the Quark-Gluon Plasma, it has an extended programme for proton–proton physics. Being the only dedicated heavy ion experiment at the CERN LHC, it was designed as the omni-purpose detector, suitable to work in a very high particle density environment. The detailed setup of ALICE can be found elsewhere [1]. Here we would like to mention, that it consists of a set of tracking and particle identification detectors, covering mainly the so-called central region $|\eta| < 0.9$, however, it contains also the forward muon spectrometer for μ pairs studies, smaller acceptance calorimeters and a number of small angle detectors. The pseudo-rapidity coverage of ALICE components is shown in Fig. 1. The ALICE physics programme covers a broad spectrum of observables, in proton–proton, proton–nucleus and nucleus–nucleus collisions at different energies. The detailed discussion can be found in [2]. The ALICE Collaboration consists of more than 1000 physicists from more than 150 institutes and 30 countries.

* Presented at the Zakopane Conference on Nuclear Physics "Extremes of the Nuclear Landscape", August 30–September 5, 2010, Zakopane, Poland.

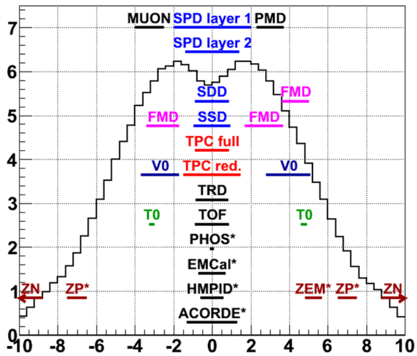

Fig. 1. Coverage of ALICE components in pseudo-rapidity η.

2. Data selection

In these studies we used data collected during the running period from December 2009 to June 2010. This contains:

$$\begin{aligned} 150\,000\ pp \text{ events at } \sqrt{s} &= 0.9 \text{ TeV;} \\ 40\,000\ pp \text{ events at } \sqrt{s} &= 2.36 \text{ TeV;} \\ 300\,000\ pp \text{ events at } \sqrt{s} &= 7 \text{ TeV.} \end{aligned}$$

The following event selection has been applied to the data:

- inelastic (INEL) events which included single diffractive (SD), non-diffractive(ND) and double diffractive (DD) events;
- non-single diffractive (NSD) events, being INEL-SD events;
- INEL>0 events, being INEL events with at least 1 charged particle within $|\eta| < 1$.

For diffractive processes, to determine systematic uncertainties in multiplicities at 0.9 and 2.36 TeV we used measured cross-sections and Monte Carlo. As the diffractive processes for 7 TeV are quite unknown, in order to minimize the model dependence we decided to use the INEL>0 event selection. Detailed discussion on data selection and applied corrections can be found in [3].

3. Multiplicity distributions

Multiplicities have been measured using the Inner Tracking System (ITS) complemented with the 2 scintillator hodoscopes, called VZERO counters. Information from VZERO counters was used for event selection and background rejection. At 0.9 TeV and 7 TeV the minimum bias trigger required a hit in either one of the VZERO counters or in the SPD detector, at 2.36 TeV, VZERO counters were turned off and the trigger required at least one hit in the SPD detector ($|\eta| < 2$). In Fig. 2 we show the mid-rapidity multiplicity density ($|\eta| < 1$) for different energies and different event selection compared with data from lower energies (left panel) and the comparison with different model predictions (right panel). It is clearly seen that the increase of the mid-rapidity multiplicity with the energy increasing from 0.9 to 7 TeV is significantly larger in the data than in Monte Carlo. Relevant numbers are given in Table I.

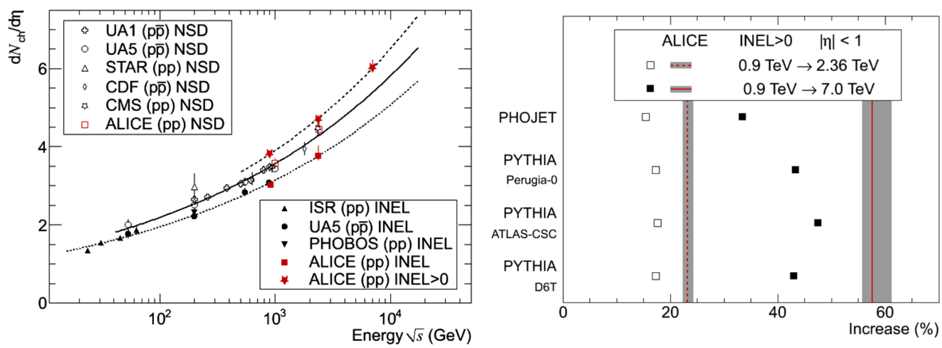

Fig. 2. Mid-rapidity multiplicity density for 0.9, 2.36 and 7 TeV, compared with data from lower energies (left panel) and the average multiplicity increase with increasing energy compared with Monte Carlo results (right panel).

TABLE I

Increase of the mid-rapidity multiplicity density, compared with Monte Carlo.

$\sqrt{s}$ increase	ALICE (%)	MC (%)
$0.9 \rightarrow 2.36$ TeV	23.3 ± 0.4	15–18
$0.9 \rightarrow 7$ TeV	57.6 ± 0.4	33–48

In Fig. 3 mid-rapidity multiplicity distributions compared with model predictions are presented. One can see that data are not reproduced by any model considered. The discrepancy does not appear to be concentrated in a single region of the distribution, and varies with the model. Fits with the negative binomial distributions (NBD) work well for 0.9 and 2.36 TeV, while at 7 TeV, the NBD fit slightly underestimates the data at low multiplicities ($N_{\mathrm{ch}} < 5$) and slightly overestimates the data at high multiplicities ($N_{\mathrm{ch}}ch > 55$) (lower right panel).

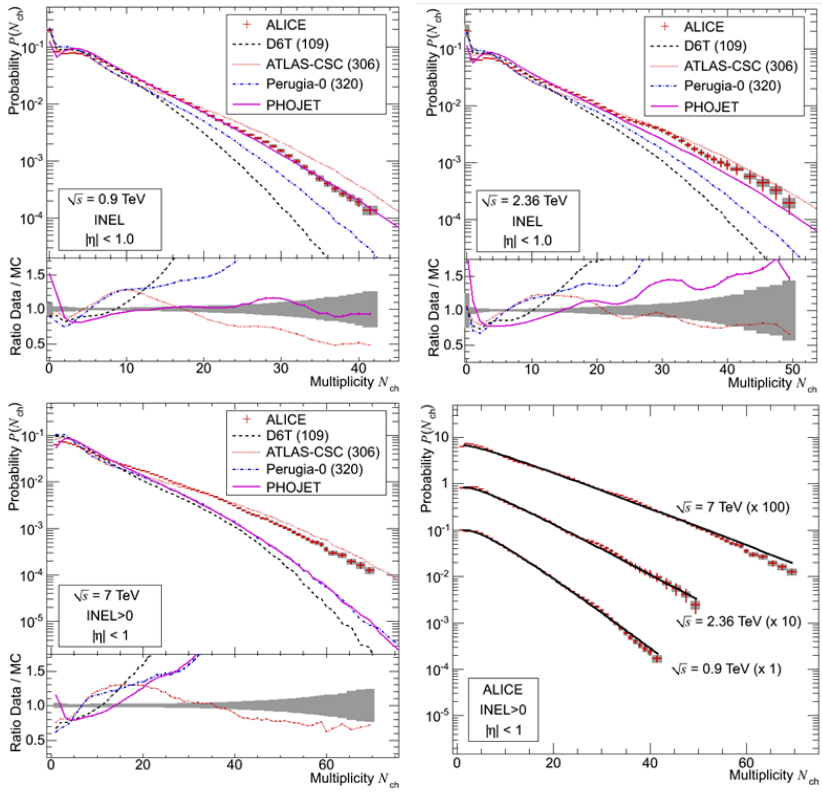

Fig. 3. Mid-rapidity multiplicity distributions for different energies compared with Monte Carlo predictions (top row and left lower panel) and fits of the negative binomial distribution to the data (lower right panel).

4. Charged particles spectra

In this section we discuss longitudinal and transverse spectra of charged particles.

4.1. Pseudo-rapidity distributions at different energies

In Fig. 4 we compare pseudo-rapidity spectra at all three energies and different event selections with different Monte Carlo predictions. As seen, none of models describe our data simultaneously for all energies.

4.2. Transverse momentum distributions at $\sqrt{s} = 0.9$ TeV

Transverse momentum spectra at $\sqrt{s} = 0.9$ TeV are shown in Fig. 5. Comparison of ALICE results, obtained for $|\eta| < 0.8$ with results obtained by other LHC experiments and by the UA5 experiment, in a broader pseudo-

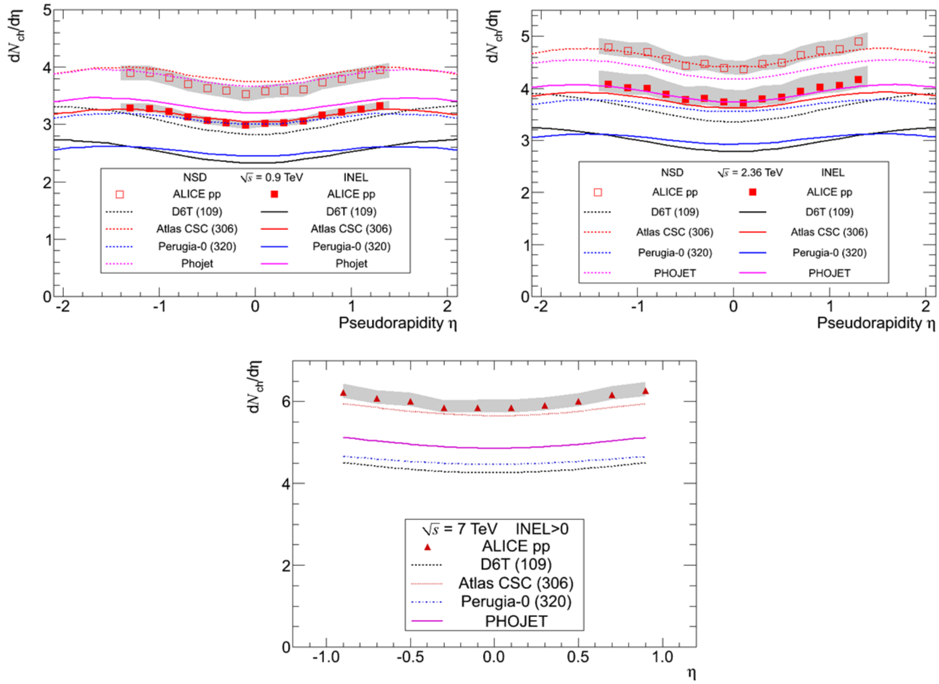

Fig. 4. Pseudo-rapidity distributions of charged particles at $\sqrt{s}$ equal to 0.9, 2.36 and 7 TeV, compared with Monte Carlo.

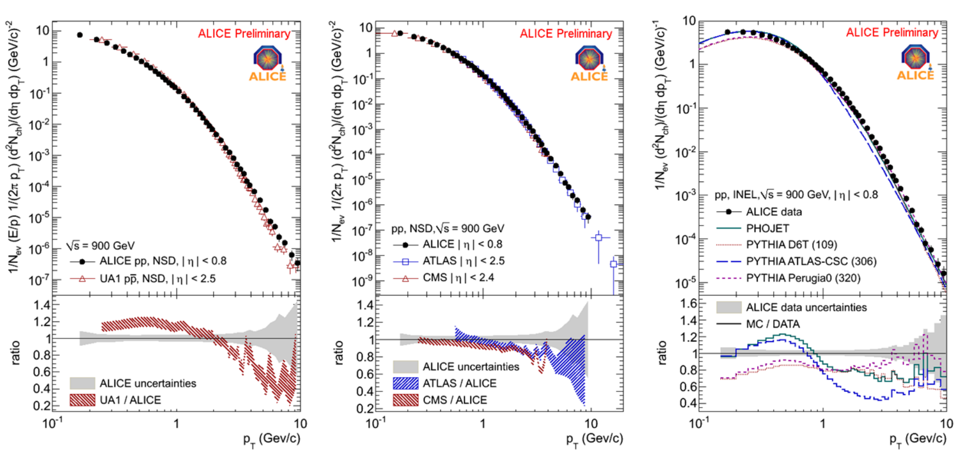

Fig. 5. Transverse momentum spectra at $\sqrt{s} = 0.9$ TeV compared with the UA1, ATLAS, CMS and Monte Carlo.

rapidity interval ($|\eta| < 2.4$–2.5), indicates that $p_{\rm t}$ spectra become harder toward mid-rapidity. We also studied transverse momentum spectra of identified particles (π, K, p), positve and negative, at $\sqrt{s} = 0.9$ TeV. Corresponding distributions are shown in Fig. 6. They are well described by the Levy function [4] of the form:

$$\frac{dN}{dp_{\rm t}} \propto p_{\rm t} \left(1 + \frac{\sqrt{m^2 + p_{\rm t}^2} - m}{nT} \right),$$

where m is a hadron mass and n, T are parameters to be fitted. This was also noticed by the STAR experiment at $\sqrt{s} = 200$ GeV [5].

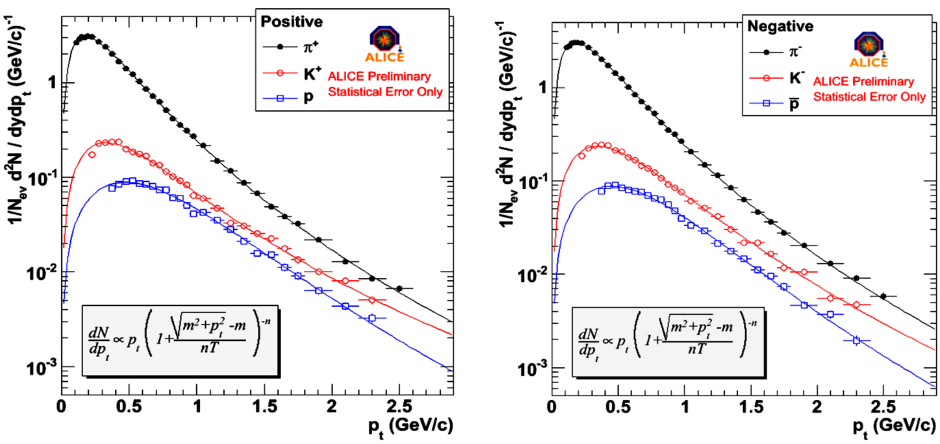

Fig. 6. Transverse momentum distributions for different particle species at $\sqrt{s} = 0.9$ TeV. Lines show the fit with Levy function.

5. Proton-to-antiproton ratio

The deceleration of the incoming proton, or more precisely of the conserved baryon number associated with the beam particles, is often called *baryon-number transport* and has been debated theoretically for some time. A brief discussion on the baryon-number transport mechanism is presented in [7]. As mentioned there, most of the (anti-) protons at mid-rapidity are created in baryon–antibaryon pair production, implying equal yields, and any excess of protons over antiprotons is therefore associated with the baryon-number transfer from the incoming beam. Model predictions for the $\overline{p}/p$ ratio at LHC energies range from unity, *i.e.*, no baryon-number transfer to mid-rapidity, down to about 0.9 in models [8], where the so-called string-junction transfer is not suppressed with the rapidity interval ($\alpha_J \approx 1$). Here we present results obtained by the ALICE experiment at

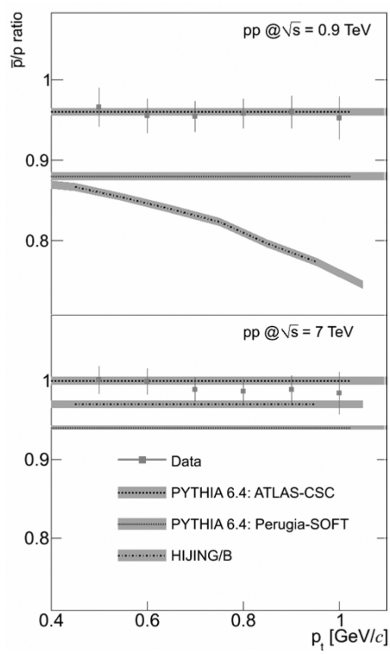

Fig. 7. Antiproton-to-proton ratio at $\sqrt{s} = 0.9$ and $\sqrt{s} = 7$ TeV.

$\sqrt{s} = 0.9$ and 7 TeV. For the analysis we selected a very central region at the pseudo-rapidity $|\eta| < 0.5$. The baryon/antibaryon identification was done using the information of their energy losses in the TPC. In Fig. 7 we show the ratio of antiprotons to protons for $\sqrt{s} = 0.9$ and $\sqrt{s} = 7$ TeV, compared with model predictions. This ratio is close to 1 at 7 TeV and within statistical errors does not depend on the transverse momentum. In Fig. 8 the $\overline{p}/p$ ratio obtained by ALICE and other experiments is plotted as a func-

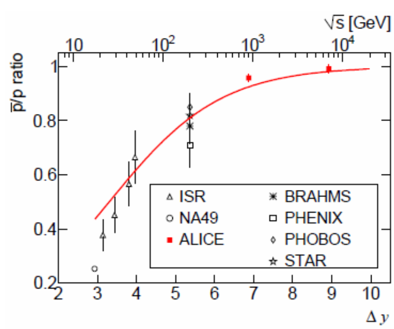

Fig. 8. Antiproton-to-proton ratio as a function of $\sqrt{s}$ (upper x-axis) and the rapidity loss Δy (lower x-axis). Solid line is described in the text.

tion of the rapidity interval $\Delta y = y_{\rm beam} - y_{\rm baryon}$, where $y_{\rm beam}$, ($y_{\rm baryon}$) is the rapidity of the incoming beam (outgoing baryon). The solid line is the rough approximation of the Δy dependence of the ratio $\overline{p}/p$ derived in the Regge model [6]. Altogether, ALICE results shown in Figs. 7 and 8, are consistent with standard models of baryon-number transport and set tight limits on any additional contributions to baryon-number transfer over very large rapidity intervals in *pp* collisions. Detailed consideration one can find in [7].

6. Summary

(i) We have shown first results on the charged particle production in *pp* collisions at $\sqrt{s} = 0.9$, 2.36, 7 TeV.

(ii) The increase of the particle density with the increase of the energy is significantly larger than in any current Monte Carlo event generator.

(iii) None of the considered models describe simultaneously the rapidity and transverse momentum distributions.

(iv) The antiproton-to-proton ration approaches 1 at the highest energy, which is consistent with standard models of baryon-number transport.

REFERENCES

[1] N. Ahmad *et al.*, CERN/LHCC/95-71(1995); G. Dellacasa *et al.*, CERN-LHCC-2000-046 (2000).

[2] [ALICE Collaboration], *J. Phys. G: Nucl. Part. Phys.* **30**, 1517 (2004); [ALICE Collaboration], *J. Phys. G: Nucl. Part. Phys.* **32**, 1295 (2006).

[3] K. Aamodt *et al.*, *Eur. Phys. J.* **C68**, 89 (2010); K. Aamodt *et al.*, *Eur. Phys. J.* **C68**, 345 (2010).

[4] [STAR Collaboration] J. Adams *et al.*, *Phys. Rev.* **C71**, 064902 (2005); G. Wilk, Z. Wlodarczyk, *Phys. Rev. Lett.* **84**, 2770 (2000).

[5] [STAR Collaboration] J. Adams *et al.*, *Phys. Lett.* **B637**, 161 (2006).

[6] D. Kharzeev, *Phys. Lett.* **B378**, 238 (1996).

[7] K. Aamodt *et al.*, *Phys. Rev. Lett.* **105**, 072002 (2010).

[8] G.C. Rossi, G. Veneziano, *Nucl. Phys.* **B123**, 507 (1977); X. Artru, *Nucl. Phys.* **B85**, 442 (1975); M. Imachi, S. Otsuki, F. Toyoda, *Prog. Theor. Phys.* **42**, 341 (1974); *Prog. Theor. Phys.* **54**, 280 (1975).